

Flatness of tracer clouds

James P. Gleeson and Dale I. Pullin

Applied Mathematics, University College Cork, Ireland. Email: j.gleeson@ucc.ie
Graduate Aeronautical Laboratories, Caltech, Pasadena, California 91125

Abstract

The average concentration of a passive scalar advected from a point source by a multivariate normal velocity field is shown to deviate from a Gaussian profile. The flatness (kurtosis) is calculated using an asymptotic series expansion valid for velocity fields with short correlation times or weak space dependence. An explicit formula for the excess flatness at first order demonstrates maximum deviation from a Gaussian profile at time t of the order of five times the velocity correlation time, with a t^{-1} decay to the Gaussian profile at large times. Monotonically decaying forms of the time correlation function are shown to yield negative values for the first order excess flatness, but positive values can result when the correlation function has an oscillatory tail.

1 Introduction

The pioneering work of Taylor [10] on dispersion problems in turbulent flows has led to the widespread use of Gaussian-plume models for the prediction of mean concentration of passive tracers or pollutants. In isotropic turbulence, for example, the mean tracer concentration may be defined as the probability distribution function (PDF) of particles released from the same point in space, with the statistical ensemble consisting of either independent experiments, or of independent particles released from the source at widely spaced time intervals. This PDF is usually assumed to have a Gaussian form, with variance determined from Taylor’s formula [3]. Taylor also argued that the Gaussian form is asymptotically correct for large times, as the particles have effectively executed a random walk through uncorrelated eddies. Moreover, if the turbulent velocity is modelled by a Gaussian (i.e., multivariate normal) velocity field, it immediately follows that the concentration is Gaussian at small times also. Thus it is only at intermediate times that any deviation from a Gaussian distribution might be observed, but few attempts have been made to examine this case.

Kraichnan [6] investigated single-particle diffusion in Gaussian velocity fields using kinematic simulations and the direct-interaction approximation (DIA). His Figure 9 shows deviations from the Gaussian distribution in numerical experiments, quantified by the flatness factor or kurtosis, which dips below its Gaussian value at intermediate times. Direct-interaction approximations of the flatness were not attempted in [6], but Koch and Shaqfeh [5] report that DIA calculations lead to an incorrect small-time limit for the flatness in a Gaussian velocity field.

Sawford and Borgas [9] investigated a variety of stochastic models for the Lagrangian velocity in turbulent flow, and showed that a multifractal model [2] and a Markovian jump model (with discontinuous velocities) both predict leptokurtic density functions, i.e., with flatness factors larger than the Gaussian value, although they note the magnitude of the deviation from the Gaussian form depends on the model chosen. Data from wind tunnel experiments is better fitted by a Gaussian distribution than by a leptokurtic distribution, although the difference is not large.

In this paper we utilize an asymptotic series expansion of the mean concentration to derive quadrature formulas for the flatness, and show that simple forms of the velocity time correlation predict a platykurtic (sub-Gaussian flatness) distribution, in agreement with Kraichnan’s numerical simulations, but contrary to the models discussed by Sawford and Borgas. The small parameter of our asymptotic series is

$$\alpha = \frac{u\tau}{L},$$

where u is the root mean square velocity, τ is the velocity correlation time, and L is an integral lengthscale. We first demonstrate that the concentration is exactly Gaussian in the limit of vanishing α : this limit corresponds to either a white-noise in time velocity field ($\tau \rightarrow 0$) [3], or to a space-independent velocity ($L \rightarrow \infty$). We then calculate the flatness using the first few terms in an asymptotic series for small α (section 2), and examine some simple examples in sections 4 and 5. In section 6, Padé approximants are used to show that the results are not restricted to infinitesimally small values of α , and we conclude with a discussion of results.

2 Exact results

The advection of a tracer from a point source at the origin by a random velocity field is described by the solution of the passive scalar equation

$$\begin{aligned} \frac{\partial}{\partial t}\theta + \nabla \cdot (\mathbf{u}\theta) &= 0, \\ \theta(\mathbf{x}, 0) &= \delta(\mathbf{x}). \end{aligned} \tag{1}$$

Here $\theta d\mathbf{x}$ is the probability, for one realization of the random velocity \mathbf{u} that a marked particle which was at the origin at time $t = 0$ will be in the volume element $d\mathbf{x}$ at time t . Taking the average over the velocity statistics yields the mean probability density function (or “concentration”) $\Theta = \langle \theta(\mathbf{x}, t) \rangle$. In isotropic turbulence the PDF Θ is a function only of time and the distance r from the source, and so $\Theta(r, t)dr$ is the probability of finding a tracer which was released at the origin at time $t = 0$ in the spherical ($d = 3$) or circular ($d = 2$) shell with radius between r and $r + dr$.

In the following, the velocity will be assumed to be isotropic, with Gaussian (multivariate normal) statistics and mean zero. The effects of molecular diffusion are ignored for clarity, so tracer particles follow the fluid exactly. It is well known that the concentration profile spreads in an approximate Gaussian shape—in particular the width of the cloud is often measured by the dispersion¹

$$D(t) = \langle r^2 \rangle = \int x_\alpha x_\alpha \Theta(\mathbf{x}, t) d\mathbf{x}, \quad (2)$$

with the integral being over all of space, and repeated indices summed from 1 to d , the number of space dimensions ($d = 2$ or 3). Taking r as the distance from the origin, we have $r = x_\alpha x_\alpha$, so $r^2 = x^2 + y^2$ in two dimensions, and $r^2 = x^2 + y^2 + z^2$ in for $d = 3$. In a previous paper [4] we addressed the calculation of the dispersion by means of an asymptotic series for small velocity correlation times and confirmed the theoretical results by calculating $\langle r^2 \rangle$ in numerical simulations. It has been noted however, that the average concentration does not have an exact Gaussian shape for all times [10, 5]. The deviation from a Gaussian shape may be measured by the flatness or kurtosis, defined as

$$f(t) = \frac{\langle r^4 \rangle}{\langle r^2 \rangle^2},$$

with $\langle r^4 \rangle$ defined similarly to (2):

$$\langle r^4 \rangle = \int x_\alpha x_\alpha x_\beta x_\beta \Theta(\mathbf{x}, t) d\mathbf{x}. \quad (3)$$

The flatness of the distribution $\Theta(\mathbf{x}, t)$ is defined as

$$f(t) = \frac{\langle r^4 \rangle}{\langle r^2 \rangle^2} = \frac{\int x_\alpha x_\alpha x_\beta x_\beta \Theta(\mathbf{x}, t) d\mathbf{x}}{\left(\int x_\alpha x_\alpha \Theta(\mathbf{x}, t) d\mathbf{x} \right)^2}. \quad (4)$$

The flatness of a d -dimensional Gaussian distribution is $(2 + d)/d$ for all times, as may be confirmed by calculating the integrals in (4) for the general isotropic distribution with zero mean and variance $\sigma^2(t)$:

$$\Theta(\mathbf{x}, t) = \frac{1}{(2\pi\sigma^2(t))^{\frac{d}{2}}} \exp\left(-\frac{x_\alpha x_\alpha}{2\sigma^2(t)}\right) \quad (5)$$

to obtain $\langle r^2 \rangle = d\sigma^2$ and $\langle r^4 \rangle = d(2 + d)\sigma^4$. Note that for a one-dimensional Gaussian distribution the corresponding flatness $\langle y^4 \rangle / \langle y^2 \rangle^2$ equals 3: it can readily be demonstrated for an isotropic distribution in d dimensions that $\langle r^2 \rangle = d\langle y^2 \rangle$ and $\langle r^4 \rangle = d\langle y^4 \rangle + d(d - 1)\langle y^2 \rangle^2$. Thus the isotropic flatness and the one-dimensional flatness are related by the equation

$$\frac{\langle r^4 \rangle}{\langle r^2 \rangle^2} = \frac{1}{d} \frac{\langle y^4 \rangle}{\langle y^2 \rangle^2} + \frac{d - 1}{d}. \quad (6)$$

¹In this paper we use the isotropic dispersion as defined in (2), which is three times the one-dimensional dispersion used in [4].

All our results are expressed in terms of the isotropic flatness.

As an example of an exactly Gaussian concentration profile, consider equation (1) when the velocity field is independent of space. The velocity statistics are then fully specified by the covariance

$$\langle u_\alpha(t)u_\beta(t') \rangle = \frac{1}{d}u^2\delta_{\alpha\beta}R(t-t').$$

We call $R(t)$ the time correlation function of the velocity; note it is symmetric about $t = 0$, with $R(0) = 1$. In this rather unusual example R must be independent of spatial arguments since the velocity depends only on time; note that in general R is defined through equation (10) below. The time correlation is usually assumed to decay to zero as t increases, with a characteristic decay time τ_* called the correlation time. The solution for the average concentration can then be shown to be precisely (5) with variance given by

$$\sigma^2(t) = 2u^2 \int_0^t \int_0^{t_1} R(t_1 - t_2) dt_1 dt_2. \quad (7)$$

As (5) is an exact Gaussian form, its flatness is $(2+d)/d$ for all time. In the following we examine how weak space dependence in the velocity field (with a finite correlation time) results in a concentration distribution with flatness less than $(2_d)/d$, and maximum deviation from the Gaussian distribution near $t = 5\tau_*$.

3 Asymptotic series expansion

We begin by Fourier-transforming all space-dependent variables such as

$$\theta(\mathbf{k}, t) = \int \theta(\mathbf{x}, t) e^{-i\mathbf{k}\cdot\mathbf{x}} d\mathbf{x}. \quad (8)$$

Henceforth only such Fourier-transformed variables are employed, so the same symbol is used as in physical space. For an isotropic, stationary and incompressible velocity field in d space dimensions, the covariance is given by

$$\langle u_\alpha(\mathbf{k}, t)u_\beta(\mathbf{p}, t') \rangle = \delta(\mathbf{k} + \mathbf{p})Q_{\alpha\beta}(\mathbf{k}, t - t'), \quad (9)$$

with

$$Q_{\alpha\beta}(\mathbf{k}, t) = \frac{E(k)R(t, k)}{2(d-1)\pi k^{d-1}} \left(\delta_{\alpha\beta} - \frac{k_\alpha k_\beta}{k^2} \right). \quad (10)$$

Here $E(k)$ is the usual energy spectrum and $R(\tau, k)$ is the time correlation function of the velocity.

Equation (1) is transformed to

$$\frac{\partial}{\partial t}\theta(\mathbf{k}, t) + i \int d\mathbf{p} \mathbf{k} \cdot \mathbf{u}(\mathbf{p}, t)\theta(\mathbf{k} - \mathbf{p}, t) = 0, \quad (11)$$

$$\theta(\mathbf{k}, 0) = 1, \quad (12)$$

which may be recast as an integral equation:

$$\theta(\mathbf{k}, t) = 1 - i \int_0^t dt_1 \int d\mathbf{p} \mathbf{k} \cdot \mathbf{u}(\mathbf{p}, t_1)\theta(\mathbf{k} - \mathbf{p}, t_1). \quad (13)$$

We seek a formal solution of (13) by iteration:

$$\begin{aligned}
\theta^{(0)} &= 1, \\
\theta^{(1)} &= 1 - i \int_0^t dt_1 \int d\mathbf{p} \mathbf{k} \cdot \mathbf{u}(\mathbf{p}, t_1) \theta^{(0)}(\mathbf{k} - \mathbf{p}, t_1) \\
&= 1 - i \int_0^t dt_1 \int d\mathbf{p} \mathbf{k} \cdot \mathbf{u}(\mathbf{p}, t_1), \\
\theta^{(2)} &= 1 - i \int_0^t dt_1 \int d\mathbf{p} \mathbf{k} \cdot \mathbf{u}(\mathbf{p}, t_1) \theta^{(1)}(\mathbf{k} - \mathbf{p}, t_1) \\
&= 1 - i \int_0^t dt_1 \int d\mathbf{p} \mathbf{k} \cdot \mathbf{u}(\mathbf{p}, t_1) \\
&\quad - \int_0^t dt_1 \int_0^{t_1} dt_2 \int d\mathbf{p} \int d\mathbf{q} \mathbf{k} \cdot \mathbf{u}(\mathbf{p}, t_1) (\mathbf{k} - \mathbf{p}) \cdot \mathbf{u}(\mathbf{q}, t_2), \\
&\vdots
\end{aligned} \tag{14}$$

We thus formally construct an infinite series solution to equation (12), involving multiple integrals over wavevectors and time. The usefulness of this approach lies in the fact that each term in the infinite series is stochastic only through the appearance of multiple velocity terms, and so the series may be averaged term-by-term to yield a series expansion for $\Theta = \langle \theta \rangle$ of the form

$$\Theta(\mathbf{k}, t) = q_0 + \alpha q_1 + \alpha^2 q_2 + \alpha^3 q_3 + \dots, \tag{16}$$

where α is a bookkeeping parameter whose power equals the number of velocity terms in the corresponding integral, q_n represents the multiple wavevector and time integrals whose integrands depend on the velocity field, and $q_0 = 1$. For a Gaussian velocity field, all even moments may be expressed in terms of the covariance (9), and all odd moments are zero:

$$q_1 = q_3 = q_5 = \dots = 0.$$

Thus q_2 , for instance, is given by

$$\begin{aligned}
q_2 &= - \int_0^t dt_1 \int_0^{t_1} dt_2 \int d\mathbf{p} \int d\mathbf{q} \langle \mathbf{k} \cdot \mathbf{u}(\mathbf{p}, t_1) (\mathbf{k} - \mathbf{p}) \cdot \mathbf{u}(\mathbf{q}, t_2) \rangle \\
&= - \int_0^t dt_1 \int_0^{t_1} dt_2 \int d\mathbf{p} \mathbf{k} \cdot \mathbf{Q}(\mathbf{p}, t_1 - t_2) \cdot (\mathbf{k} - \mathbf{p}) \\
&= - \int_0^t dt_1 \int_0^{t_1} dt_2 \int d\mathbf{p} \mathbf{k} \cdot \mathbf{Q}(\mathbf{p}, t_1 - t_2) \cdot \mathbf{k},
\end{aligned} \tag{17}$$

where we have used (9) and the incompressibility of the velocity field. Contributions to q_4 come from the average of four velocity terms, which factors to yield

$$\begin{aligned}
q_4 &= \int_0^t dt_1 \int_0^{t_1} dt_2 \int_0^{t_2} dt_3 \int_0^{t_3} dt_4 \int d\mathbf{p} \int d\mathbf{q} [\mathbf{k} \cdot \mathbf{Q}(\mathbf{p}, t_1 - t_2) \cdot \mathbf{k}] [\mathbf{k} \cdot \mathbf{Q}(\mathbf{q}, t_3 - t_4) \cdot \mathbf{k}] \\
&+ \int_0^t dt_1 \int_0^{t_1} dt_2 \int_0^{t_2} dt_3 \int_0^{t_3} dt_4 \int d\mathbf{p} \int d\mathbf{q} [\mathbf{k} \cdot \mathbf{Q}(\mathbf{p}, t_1 - t_3) \cdot (\mathbf{k} - \mathbf{q})] [(\mathbf{k} - \mathbf{p}) \cdot \mathbf{Q}(\mathbf{q}, t_2 - t_4) \cdot \mathbf{k}] \\
&+ \int_0^t dt_1 \int_0^{t_1} dt_2 \int_0^{t_2} dt_3 \int_0^{t_3} dt_4 \int d\mathbf{p} \int d\mathbf{q} [\mathbf{k} \cdot \mathbf{Q}(\mathbf{p}, t_1 - t_4) \cdot \mathbf{k}] [(\mathbf{k} - \mathbf{p}) \cdot \mathbf{Q}(\mathbf{q}, t_2 - t_3) \cdot (\mathbf{k} - \mathbf{p})] \\
&\dots
\end{aligned} \tag{18}$$

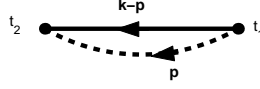


Figure 1: Diagram of order 1.

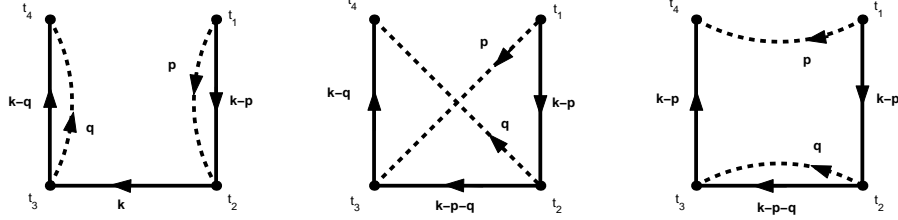


Figure 2: The three diagrams of order 2.

The factorisation of averages of the Gaussian field into products of velocity covariances leads to a sum of $(2n)!/2^n n!$ terms contributing to q_{2n} .

We remark here that the various terms may be accounted for using a diagram expansion method, such as is commonly employed in perturbation expansions over Gaussian fields [8]. First, define the diagrams of order n to be $2n$ -polygons with dotted lines joining pairs of vertices. For example, the diagram of order 1 representing equation (17) is shown in Figure 1, with the three diagrams of order 2 (representing q_4) in Figure 2. The expressions for the q_{2n} may be recovered from the diagrams of order n by applying the following diagram rules. Consider the middle diagram of Figure 2, which represents the second term on the right hand side of (18):

$$\int_0^t dt_1 \int_0^{t_1} dt_2 \int_0^{t_2} dt_3 \int_0^{t_3} dt_4 \int d\mathbf{p} \int d\mathbf{q} [(\mathbf{k} - \mathbf{p}) \cdot \mathbf{Q}(\mathbf{p}, t_1 - t_3) \cdot (\mathbf{k} - \mathbf{q})] \times \\ \times [(\mathbf{k} - \mathbf{p} - \mathbf{q}) \cdot \mathbf{Q}(\mathbf{q}, t_2 - t_4) \cdot \mathbf{k}]. \quad (19)$$

Observe that (19) may be deduced from the diagram by applying the following rules:

1. Vertex labels are the time integration variables.
2. The wavevector integration variables are the wavevectors labeling the internal dotted lines; these integrals are over all wavevector space.
3. The vector sum of wavevectors at each vertex is zero, except for the first vertex (labeled t_1) which has sum $+\mathbf{k}$, and the final vertex which has sum $-\mathbf{k}$.

To compose the integrand, we multiply the factors resulting from each of the following rules:

4. For each internal dotted line, consider the start and end vertices. In the diagram example above, for the internal dotted line labeled \mathbf{p} , the start vertex is labeled t_1 and the end vertex is labeled t_3 . Both the start and the end vertex have solid lines emanating from them; suppose the wavevector labels on these lines are \mathbf{a} and \mathbf{b} respectively. Then the factor we seek is $-\mathbf{a} \cdot \mathbf{Q}(\mathbf{p}, t_s - t_e) \cdot \mathbf{b}$ where \mathbf{p} is the dotted line label and t_s and t_e are the start and end vertex labels. (If the end vertex is the circled vertex, then let $\mathbf{b} = \mathbf{k}$). In the example, $\mathbf{a} = \mathbf{k} - \mathbf{p}$ and $\mathbf{b} = \mathbf{k} - \mathbf{q}$, so that the factor is $-(\mathbf{k} - \mathbf{p}) \cdot \mathbf{Q}(\mathbf{p}, t_1 - t_3) \cdot (\mathbf{k} - \mathbf{q})$. By applying this rule again to the second dotted line, we find another factor of $-(\mathbf{k} - \mathbf{p} - \mathbf{q}) \cdot \mathbf{Q}(\mathbf{q}, t_2 - t_4) \cdot \mathbf{k}$. Further simplification may be possible due to incompressibility.

These rules form an algorithm for finding the q_{2n} terms in the iteration expansion of Θ and so may be implemented using a symbolic manipulation program like *Mathematica*.

The behaviour of each diagram as time increases determines the quality of the approximation to Θ resulting from truncating the infinite series. If the time correlation function $R(t, k)$ decays sufficiently quickly (e.g., exponentially) to zero as $t \rightarrow \infty$, it can be shown that *connected* diagrams, i.e., those which cannot be split into two separate parts by cutting one solid line, grow linearly in time and so their contribution to $\partial\Theta/\partial t$ remains bounded as $t \rightarrow \infty$. On the other hand, *unconnected diagrams* such as the first term on the right hand side of (18) grow faster than linearly, and their contribution to $\partial\Theta/\partial t$ is unbounded. With a view to renormalising the infinite series (16) to eliminate these secular effects, we make the ansatz that the evolution of the PDF Θ may be described by the simple differential equation

$$\frac{\partial\Theta}{\partial t} = K(\mathbf{k}, t)\Theta(\mathbf{k}, t), \quad (20)$$

with the factor K to be determined. This ansatz leads effectively to a cumulant expansion [8]. This renormalisation is not unique, for instance the functional-derivative closure (FDC) method advanced in [4] leads to an integrodifferential equation

$$\frac{\partial\Theta}{\partial t} = \int_0^t K(\mathbf{k}, s)\Theta(\mathbf{k}, s)ds, \quad (21)$$

and eventually to results identical to those presented here, but with significantly more effort. Noting that the solution to (20) satisfying the initial condition is

$$\Theta(\mathbf{k}, t) = \exp \left[\int_0^t K(\mathbf{k}, T)dT \right], \quad (22)$$

it remains only to find an expression for K as a cumulant expansion.

We seek an expansion for K in even powers of α :

$$K = K_0 + \alpha^2 K_2 + \alpha^4 K_4 + \dots \quad (23)$$

and utilise this and (16) in (20) to match coefficients of powers of α term-by-term

$$\alpha^2 \frac{\partial q_2}{\partial t} + \alpha^4 \frac{\partial q_4}{\partial t} + \dots = (K_0 + \alpha^2 K_2 + \alpha^4 K_4 + \dots) (q_0 + \alpha^2 q_2 + \alpha^4 q_4 + \dots), \quad (24)$$

yielding the K_n in terms of the known q_n :

$$\begin{aligned} K_0 &= 0, \\ K_2 &= \frac{1}{q_0} \frac{\partial q_2}{\partial t} \\ K_4 &= \frac{1}{q_0} \left[\frac{\partial q_4}{\partial t} - \frac{q_2}{q_0} \frac{\partial q_2}{\partial t} \right] \\ &\vdots \end{aligned} \quad (25)$$

Thus, for example, K_2 is found from (17) to be

$$K_2 = - \int_0^t dt_2 \int d\mathbf{p} \mathbf{k} \cdot \mathbf{Q}(\mathbf{p}, t - t_2) \cdot \mathbf{k}, \quad (26)$$

and again, each K_n may be calculated using symbolic manipulation computer packages. Moreover, it is found that the undesirable growth of terms as $t \rightarrow \infty$ noted above is not present in the expansion for K , thus allowing us to use (22) as an approximation to Θ over all time.

Having found an expansion for the probability density function of tracers (22), it remains only to use this to calculate the flatness of the distribution, according to equation (4). In terms of the Fourier transformed variables, the moments such as (3) may be written as

$$\langle r^4 \rangle = \frac{\partial^4}{\partial k_\alpha \partial k_\alpha \partial k_\beta \partial k_\beta} \Theta(\mathbf{k}, t) \Big|_{\mathbf{k}=\mathbf{0}}, \quad (27)$$

and for an isotropic distribution (i.e., Θ depending only on magnitude k of \mathbf{k} , independent of orientation) in d dimensions this reduces to

$$\langle r^4 \rangle = \frac{d(2+d)}{3} \frac{\partial^4}{\partial k^4} \Theta(k, t) \Big|_{k=0}. \quad (28)$$

Similarly, the isotropic second moment is

$$\langle r^2 \rangle = -d \frac{\partial^2}{\partial k^2} \Theta(k, t) \Big|_{k=0},$$

and so the flatness (4) is

$$f(t) = \frac{2+d}{3d} \frac{\frac{\partial^4 \Theta}{\partial k^4} \Big|_{k=0}}{\left(-\frac{\partial^2 \Theta}{\partial k^2} \Big|_{k=0} \right)^2}, \quad (29)$$

which is written in terms of K using (22):

$$f(t) = \frac{2+d}{3d} \left[3 + \frac{\frac{\partial^4}{\partial k^4} \int_0^t K(k, T) dT \Big|_{k=0}}{\left(-\frac{\partial^2}{\partial k^2} \int_0^t K(k, T) dT \Big|_{k=0} \right)^2} \right]. \quad (30)$$

Using the expansion (23) of K derived above, it is straightforward to calculate the derivatives in (30) term-by-term; for convenience we introduce the notation

$$\begin{aligned} D_n &= -\frac{\partial^2}{\partial k^2} \int_0^t K_n(k, T) dT \Big|_{k=0} \\ F_n &= \frac{\partial^4}{\partial k^4} \int_0^t K_n(k, T) dT \Big|_{k=0} \end{aligned} \quad (31)$$

and so (30) becomes

$$f(t) = \frac{2+d}{3d} \left[3 + \frac{\sum_{n=1}^{\infty} \alpha^{2n} F_{2n}(t)}{\left(\sum_{n=1}^{\infty} \alpha^{2n} D_{2n}(t) \right)^2} \right]. \quad (32)$$

Noting that $F_2 = F_4 = 0$, we list in the appendix F_6 and D_2 to D_6 , having performed all angular integrals, and so reducing the expressions to multiple integrals over time and wavenumbers.

4 Exponential time correlation

As a further simplification we now take the time correlation function to have the following form:

$$R(t, k) = e^{-\omega|t|}. \quad (33)$$

This is a rather unrealistic approximation to the time correlation of turbulent velocity fields, chiefly because it is not differentiable at $t = 0$, and also due to its lack of dependence on the wavenumber k (see [4, 7]).

However, it results in a number of simplifications of our analysis which enable the structure of the expansion to be clearly shown; we note further that numerical computation by quadrature is always possible in the general case. Such a quadrature computation is performed for a correlation function which is smooth at $t = 0$ in the next section, and the flatness behaves similarly to the analytical results derived here.

With R independent of wavenumber, the integrals over p , q and r reduce to moments of the energy spectrum, for which we introduce the notation

$$m_i = \frac{d-1}{d} \int_0^\infty k^i E(k) dk. \quad (34)$$

The factor of $(d-1)/d$ ensures the simple identification $m_0 = u^2$. Note that if R is wavenumber-dependent, then the full quadrature expressions given in the appendix must be evaluated, whereas assuming R to depend only on the time difference allows us to evaluate all wavenumber integrals in terms of the moments (34) of the energy spectrum.

We now nondimensionalise variables by a characteristic wavenumber k_0 and the correlation time ω^{-1} , and note that the bookkeeping parameter emerges naturally as the nondimensional number

$$\alpha = \frac{uk_0}{\omega}.$$

Further simplification follows by using (33) and introducing the Laplace transform

$$\tilde{D}(s) = \int_0^\infty e^{-st} D(t) dt,$$

so that the series expansion of the dispersion $D(t)$ transforms to

$$\tilde{D}(s) = \alpha^2 \tilde{D}_2(s) + \alpha^4 \tilde{D}_4(s) + \dots, \quad (35)$$

with

$$\tilde{D}_2(s) = 2u^2 \frac{1}{s^2(s+1)} \quad (36)$$

and

$$\tilde{D}_4(s) = -2u^2 m_2 \frac{1}{s^2(s+1)^2(s+2)}. \quad (37)$$

Similarly, the Laplace transform of the fourth tracer moment is

$$\tilde{F}(s) = \alpha^2 \tilde{F}_2(s) + \alpha^4 \tilde{F}_4(s) + \alpha^6 \tilde{F}_6(s) + \dots, \quad (38)$$

with

$$\tilde{F}_2(s) = \tilde{F}_4(s) = 0 \quad (39)$$

and, for $d = 3$,

$$\tilde{F}_6^{3D}(s) = -\frac{144u^4 m_2 (5s+8)}{5s^2(s+1)^3(s+2)^2(s+3)}. \quad (40)$$

The two-dimensional versions of D have the same form as above, but the F_6 term must be multiplied by $5/4$ to go from the three dimensional (40) to the two-dimensional equivalent:

$$\tilde{F}_6^{2D}(s) = -\frac{36u^4 m_2 (5s+8)}{s^2(s+1)^3(s+2)^2(s+3)}. \quad (41)$$

Each of the series may be viewed as asymptotic expansions about $\alpha = 0$, as they are clearly power series in even powers of α . Recalling the definition of α as uk_0/ω , we identify the $\alpha \rightarrow 0$ limit as the limit

of small correlation time (white noise in time, $\omega \rightarrow \infty$), or of a weak space dependence of the velocity field ($k_0 \rightarrow 0$). The latter interpretation is related to the exact solution discussed in section 2. We showed that a velocity field that depends only on time leads to a tracer concentration which is exactly Gaussian. Being independent of space means that the energy spectrum is a delta function: $E(k) \propto \delta(k)$, so all moments m_n are zero and all terms in the series for F vanish identically.

The limiting behaviour of $D_n(t)$ and $F_n(t)$ as $t \rightarrow 0$ may be found by inverting the Laplace transform, or more simply by expanding the transforms $\tilde{D}_n(s)$ and $\tilde{F}_n(s)$ about $s = \infty$, then reading off the coefficient of t^n as $1/n!$ times the coefficient of $s^{-(n+1)}$. We find

$$D_2(t) = u^2 t^2 + O(t^3), \quad (42)$$

$$D_4(t) = -\frac{1}{12} u^4 m_2 t^4 + O(t^5), \quad (43)$$

$$F_6^{3D}(t) = -\frac{1}{5} u^4 m_2 t^6 + O(t^7) \text{ as } t \rightarrow 0, \quad (44)$$

$$F_6^{2D}(t) = -\frac{1}{4} u^4 m_2 t^6 + O(t^7) \text{ as } t \rightarrow 0, \quad (45)$$

and in general

$$\begin{aligned} D_{2n}(t) &= O(t^{2n}), \\ F_{2n}(t) &= O(t^{2n}) \text{ as } t \rightarrow 0. \end{aligned} \quad (46)$$

Similarly the limit as $t \rightarrow \infty$ may be found without inverting the Laplace transform by expanding it into partial fractions of the form

$$\frac{A_1}{s^2} + \frac{A_2}{s} + \sum_{i=1}^l \frac{B_i}{(s - b_i)^{n_i}} + \dots, \quad (47)$$

which inverts to

$$A_1 t + A_2 + \text{exponentially decaying terms},$$

provided that the poles b_i all have negative real part. Using this, we find

$$D_2(t) = 2u^2 t + o(t), \quad (48)$$

$$D_4(t) = -u^2 m_2 t + o(t), \quad (49)$$

$$F_6^{3D}(t) = -\frac{96}{5} u^4 m_2 t + o(t) \text{ as } t \rightarrow \infty, \quad (50)$$

$$F_6^{2D}(t) = -24u^4 m_2 t + o(t) \text{ as } t \rightarrow \infty, \quad (51)$$

with the general result being

$$\begin{aligned} D_n(t) &= O(t), \\ F_n(t) &= O(t) \text{ as } t \rightarrow \infty. \end{aligned} \quad (52)$$

Consider the flatness when $\alpha \ll 1$, i.e., when the correlation time is short or the velocity is only weakly space-dependent. Then we approximate F and D by the first non-zero terms in their expansions:

$$\begin{aligned} D(t) &\approx \alpha^2 D_2(t), \\ F(t) &\approx \alpha^6 F_6(t), \end{aligned}$$

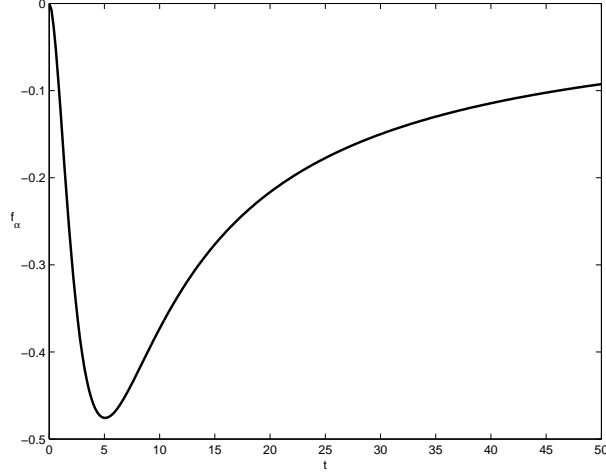


Figure 3: First order excess flatness (53) for exponential time correlation.

and find the flatness from (32) to be

$$f(t) \approx \frac{2+d}{3d} \left[3 + \alpha^2 \frac{F_6(t)}{(D_2(t))^2} \right].$$

As the limit $\alpha \rightarrow 0$ corresponds to the exactly Gaussian case, we define the *excess flatness* as

$$f_\alpha(t) = \frac{1}{m_2} \frac{F_6(t)}{(D_2(t))^2}. \quad (53)$$

From the limits discussed above, it is clear that the excess flatness approaches zero as $t \rightarrow 0$ and as $t \rightarrow \infty$. Inverting (39) and (40) yields an analytical expression for the excess flatness:

$$f_\alpha^{3D}(t) = \frac{-2(24t - 89) - 7e^{-3t} - 18(2t + 1)e^{-2t} - 9(6t^2 + 14t + 17)e^{-t}}{10(t - 1 + e^{-t})^2}. \quad (54)$$

The corresponding two-dimensional value is obtained by multiplying (54) by 5/4. The minimum near $t = 5$ (see Figure 3) is accurately determined numerically to demonstrate that the maximum deviation from the Gaussian flatness occurs at (dimensional) time

$$t = 5.0630\omega^{-1}, \quad (55)$$

with flatness

$$\begin{aligned} f^{3D} &= \frac{5}{9} [3 + \alpha^2 m_2 f_\alpha^{3D}(5.0630)] \\ &= \frac{5}{3} - 0.264346\alpha^2 m_2. \end{aligned} \quad (56)$$

Similarly, the two-dimensional minimum flatness is

$$f^{2D} = 2 - 0.396518\alpha^2 m_2. \quad (57)$$

As $t \rightarrow \infty$, the excess flatness returns to zero from below; its asymptotic form can be found readily from (54), or using (48) and (50) to be

$$f_\alpha^{3D}(t) \sim -\frac{24}{5} \frac{1}{t} + o\left(\frac{1}{t}\right) \text{ as } t \rightarrow \infty, \quad (58)$$

$$f_\alpha^{2D}(t) \sim -\frac{6}{t} + o\left(\frac{1}{t}\right) \text{ as } t \rightarrow \infty. \quad (59)$$

5 Other time correlation functions

It is possible to relax the assumption (33) on the time correlation function to permit an oscillatory tail:

$$R(t, k) = e^{-\omega|t|} \cos(at). \quad (60)$$

The Laplace transform techniques of the previous section are also applicable here, and the excess flatness may again be expressed as (53), with D_2 and F_6 given in terms of their Laplace transforms for brevity:

$$\begin{aligned} \tilde{D}_2(s) &= -\frac{2u^2(s+1)}{s^2[(s+1)^2+a^2]}, \\ \tilde{F}_6^{3D}(s) &= \frac{48u^4m_2}{5s^2(s+2)^2[(s+1)^2+a^2]^3[(s+2)^2+4a^2]^2[(s+3)^2+a^2][(s+3)^2+9a^2]} \times \\ &\quad \times [36a^{10}s - 3(2+s)^4(8+5s)(3+4s+s^2)^3 + 5a^8s(168+108s+23s^2) \\ &\quad + a^6(3456+14832s+18388s^2+9533s^3+2160s^4+189s^5) \\ &\quad - a^2(2+s)^2(-4896-16203s-20820s^2-12701s^3-3222s^4+181s^5+250s^6+35s^7) \\ &\quad + a^4(33408+121032s+178036s^2+137633s^3+60112s^4+14707s^5+1842s^6+90s^7)]. \end{aligned}$$

In two dimensions, the D_2 term is as above, whereas the F_6^{2D} term is 5/4 times the three-dimensional version.

Using the Laplace transforms to find the asymptotic behaviour yields

$$f_\alpha^{3D}(t) \sim -\frac{24}{5} \frac{1-3a^2}{(1+a^2)^3} \frac{1}{t} + o\left(\frac{1}{t}\right) \text{ as } t \rightarrow \infty,$$

which reduces to (58) at $a = 0$. A similar generalization of (59) holds in two dimensions. Note that the excess flatness decays to zero from above if $a > 1/\sqrt{3}$. This behaviour, and the appearance of oscillations in $f_\alpha(t)$ are shown in Figure 4.

As a final example of the $O(\alpha^2)$ excess flatness, we consider the time correlation function

$$R(t, k) = e^{-\frac{\omega^2 t^2}{2}}. \quad (61)$$

In this case the time integrals must be calculated numerically; see Figure 5 for the three-dimensional case. Again, the two-dimensional flatness is 5/4 times the three-dimensional value. Note the negative excess near $t = 5$ and slow return to zero excess flatness as $t \rightarrow \infty$, similar to that found analytically for the exponential time correlation function. We conclude that the properties of the flatness demonstrated in the previous section are not strongly dependent upon the smoothness of R at $t = 0$.

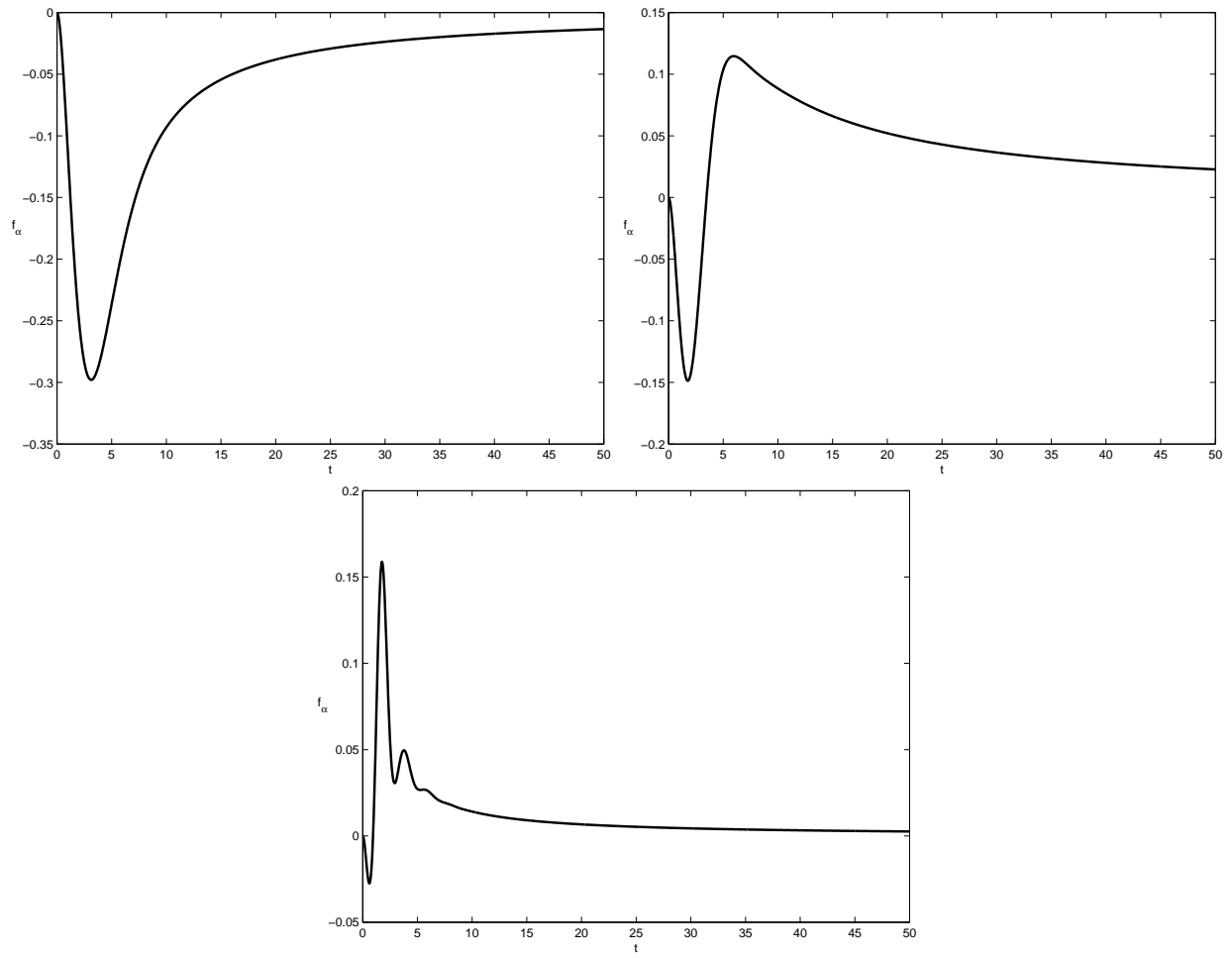


Figure 4: First order excess flatness for oscillatory time correlation, for various values of a : (i) $a = 0.5$, (ii) $a = 1$, (iii) $a = 3$.

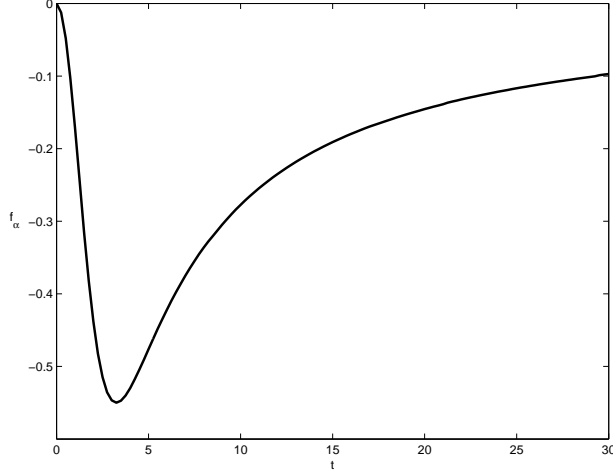


Figure 5: First order excess flatness in three dimensions for time correlation function (61).

6 Single-scale field: Padé approximants

In order to extend the analysis to include higher powers of α , it is convenient to adopt the exponential time correlation function (33) and a single-scale (dimensional) energy spectrum

$$E(k) = \frac{d}{d-1} u^2 \delta(k - k_0), \quad (62)$$

which allows us to set all moments of the energy spectrum to unity, $m_n = 1$ (having nondimensionalised with k_0 and ω as before).

Even with this simplification, the higher order terms involve significant symbolic manipulation, and are most succinctly expressed in terms of their Laplace transforms:

$$\begin{aligned} \tilde{D}_6^{3D}(s) &= \frac{11 + 7s}{s^2(s+1)^3(s+2)^2(s+3)}, \\ \tilde{D}_8^{3D}(s) &= -\frac{8122 + 14299s + 8332s^2 + 1555s^3}{25s^2(s+1)^4(s+2)^3(s+3)^2(s+4)}, \\ \tilde{F}_8^{3D}(s) &= \frac{432(1202 + 2070s + 1184s^2 + 217s^3)}{25s^2(s+1)^4(s+2)^3(s+3)^2(s+4)}, \\ \tilde{F}_{10}^{3D}(s) &= -\frac{24(38048360 + 120925228s + 159153150s^2 + 109999511s^3)}{125s^2(s+1)^5(s+2)^4(s+3)^3(s+4)^2(s+5)} \\ &\quad - \frac{24(41758657s^4 + 8215311s^5 + 652275s^6)}{125s^2(s+1)^5(s+2)^4(s+3)^3(s+4)^2(s+5)}. \end{aligned}$$

In two dimensions:

$$\begin{aligned}
\tilde{D}_6^{2D}(s) &= \frac{19 + 11s}{2s^2(s+1)^3(s+2)^2(s+3)}, \\
\tilde{D}_8^{2D}(s) &= -\frac{241 + 402s + 227s^2 + 42s^3}{s^2(s+1)^4(s+2)^3(s+3)^2(s+4)}, \\
\tilde{F}_8^{2D}(s) &= \frac{6(4410 + 7559s + 4318s^2 + 791s^3)}{s^2(s+1)^4(s+2)^3(s+3)^2(s+4)}, \\
\tilde{F}_{10}^{2D}(s) &= -\frac{3(3063840 + 9668828s + 12679606s^2 + 8752083s^3)}{s^2(s+1)^5(s+2)^4(s+3)^3(s+4)^2(s+5)} \\
&\quad - \frac{3(3322145s^4 + 653857s^5 + 51945s^6)}{s^2(s+1)^5(s+2)^4(s+3)^3(s+4)^2(s+5)}.
\end{aligned}$$

Having calculated these higher order terms in the asymptotic series, we use Padé approximants [1] to accelerate convergence of the asymptotic series. We note that such methods were used successfully in [4] for the related problem of calculating turbulent diffusivities. Padé approximants to D and F are defined as rational functions of α which yield the same asymptotic series for small α :

$$\begin{aligned}
D^{[0,0]}(t) &= D_2(t), \\
D^{[0,1]}(t) &= \frac{D_2(t)}{1 - \alpha^2 \frac{D_4(t)}{D_2(t)}}, \\
D^{[1,1]}(t) &= \frac{D_2 + \alpha^2 \frac{D_4^2 - D_2 D_6}{D_4}}{1 - \alpha^2 \frac{D_6}{D_4}}, \\
F^{[0,0]}(t) &= F_6(t), \\
F^{[0,1]}(t) &= \frac{F_6(t)}{1 - \alpha^2 \frac{D_8(t)}{D_6(t)}}, \\
F^{[1,1]}(t) &= \frac{F_6 + \alpha^2 \frac{F_8^2 - F_6 F_{10}}{F_8}}{1 - \alpha^2 \frac{F_{10}}{F_8}}.
\end{aligned}$$

The excess flatness is thus successively approximated by

$$\begin{aligned}
f^{[0,0]} &= \frac{F^{[0,0]}}{(D^{[0,0]})^2}, \\
f^{[0,1]} &= \frac{F^{[0,1]}}{(D^{[0,1]})^2}, \\
f^{[1,1]} &= \frac{F^{[1,1]}}{(D^{[1,1]})^2},
\end{aligned}$$

and yields curves that lie close together for α on the order of $1/2$, see Figures 6 and 7 for the three- and two-dimensional cases, respectively. The fact that successive Padé approximants lie close together may heuristically be taken to indicate that the exact value of the excess flatness is indeed negative even when α is not infinitesimally small, and so the PDF Θ is platykurtic (has sub-Gaussian flatness). This is supported by the numerical simulations of Kraichnan [6], which are performed at relatively high values of α , and is contrary to the predictions of the multifractal and Markovian jump models examined by Sawford and Borgas [9].

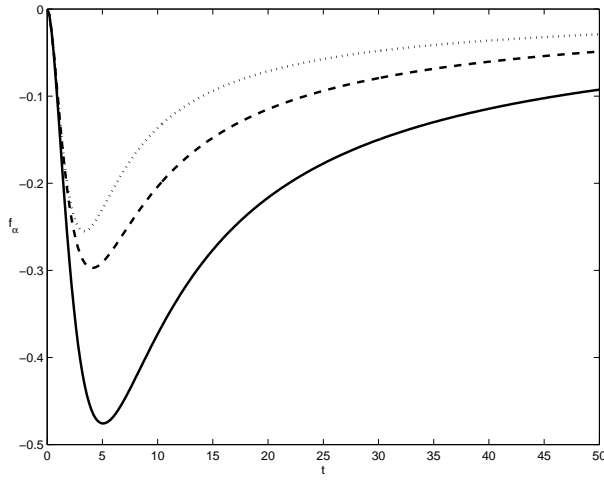


Figure 6: Padé approximants $f^{[0,0]}$ (solid), $f^{[0,1]}$ (dashed), and $f^{[1,1]}$ (dotted) in three dimensions, with $\alpha = 0.75$.

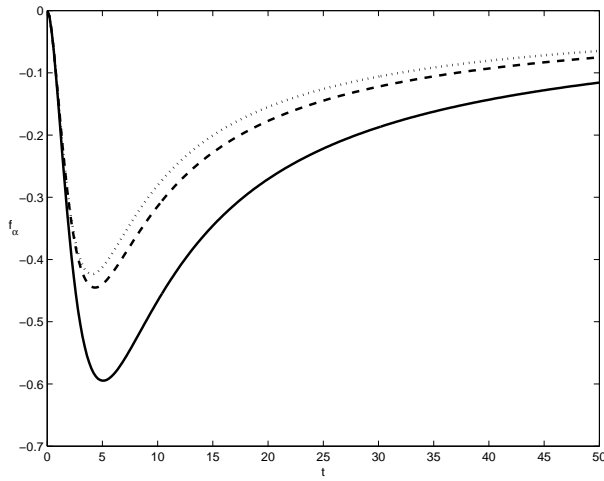


Figure 7: Padé approximants $f^{[0,0]}$ (solid), $f^{[0,1]}$ (dashed), and $f^{[1,1]}$ (dotted) in two dimensions, with $\alpha = 0.5$.

7 Conclusion

We have described an asymptotic series expansion for the PDF of tracers (i.e., mean concentration field) advected by a Gaussian random velocity field in the form of a cumulant expansion. As noted following equation (20), the renormalisation procedure which ensures that the series is non-secular in time is not unique, but the approach taken here is algebraically simpler than, for instance, the FDC method of [4], and leads to the same results.

Our main result is equation (32) for the tracer flatness along with the quadrature expressions for D_n and F_n given in the Appendix. In principle, these imply that the tracer flatness is fully specified once the energy spectrum and the time correlation function R of the velocity field are given. We have examined some particularly interesting examples in sections 4 through 6, which include an analytic formula (54) for the flatness when R is an exponential function, and a generalisation to the case where R has an oscillatory tail (section 4). Numerical quadrature for a smooth monotonic R yields similar results to the analytical expression (54), and Padé approximants extend the result beyond infinitesimal values of α , at least for the single-scale energy spectrum (62).

The conclusion to be drawn from Figures 3, 5 and 6 and the formulas for F_6 in the Appendix is that the tracer PDF is platykurtic (i.e., has negative excess flatness) when the velocity correlation function R is monotonically decaying in time, at least for low values of the parameter α . This conclusion is supported by Kraichnan's numerical simulations for finite values of α [6], but contradicts the predictions of two models in [9]. Interestingly, the excess flatness can exhibit positive values when R has an oscillatory tail, see Figure 4. It would be interesting to extend Kraichnan's numerical simulations to examine such cases. Further work is also required to calculate the flatness when R depends non-trivially on the wavenumber as well as on the time difference.

8 Acknowledgements

This project was partly funded by the Enterprise Ireland International Collaboration Fund, and by a research grant from the Faculty of Arts, University College Cork.

A Appendix

The asymptotic series expansion detailed in section 3 leads to expression (31) for the flatness, involving multiple integrals over wavevectors and time. The angular integrals may be performed exactly, and so the reduced forms for the isotropic D_{2n} and F_{2n} for $n \leq 3$ in three dimensions are as follows. Note that these expressions include general wavenumber dependence in the time correlation function R ; further simplification follows when wavenumber-independent correlation functions are considered as in sections 4

through 6.

$$\begin{aligned}
D_2^{3D} &= \frac{4}{3} \int_0^t dt_1 \int_0^{t_1} dt_2 \int_0^\infty dp E(p) R(t_1 - t_2, p) \\
D_4^{3D} &= -\frac{8}{9} \int_0^t dt_1 \int_0^{t_1} dt_2 \int_0^{t_2} dt_3 \int_0^{t_3} dt_4 \int_0^\infty dp \int_0^\infty dq p^2 E(p) E(q) R(t_1 - t_4, p) R(t_2 - t_3, q) \\
D_6^{3D} &= \int_0^\infty dp \int_0^\infty dq \int_0^\infty dr \int_0^t dt_1 \int_0^{t_1} dt_2 \int_0^{t_2} dt_3 \int_0^{t_3} dt_4 \int_0^{t_4} dt_5 \int_0^{t_5} dt_6 E(p) E(q) E(r) \times \\
&\quad \times \left[\frac{16p^4}{27} R(t_1 - t_6, p) R(t_2 - t_5, q) R(t_3 - t_4, r) + \right. \\
&\quad \quad \frac{16p^2q^2}{27} R(t_1 - t_6, p) R(t_2 - t_5, q) R(t_3 - t_4, r) + \\
&\quad \quad \frac{16p^4}{27} R(t_1 - t_6, p) R(t_2 - t_4, q) R(t_3 - t_5, r) + \\
&\quad \quad \frac{16p^4}{27} R(t_1 - t_6, p) R(t_2 - t_3, q) R(t_4 - t_5, r) - \\
&\quad \quad \frac{16p^2q^2}{135} R(t_1 - t_5, p) R(t_2 - t_6, q) R(t_3 - t_4, r) - \\
&\quad \quad \frac{8p^2q^2}{135} R(t_1 - t_4, p) R(t_2 - t_6, q) R(t_3 - t_5, r) - \\
&\quad \quad \frac{8p^2r^2}{135} R(t_1 - t_5, p) R(t_2 - t_4, q) R(t_3 - t_6, r) - \\
&\quad \quad \left. \frac{8p^2r^2}{135} R(t_1 - t_4, p) R(t_2 - t_5, q) R(t_3 - t_6, r) \right]
\end{aligned}$$

$$F_2^{3D} = 0$$

$$F_4^{3D} = 0$$

$$\begin{aligned}
F_6^{3D} &= -\frac{64}{45} \int_0^\infty dp \int_0^\infty dq \int_0^\infty dr \int_0^t dt_1 \int_0^{t_1} dt_2 \int_0^{t_2} dt_3 \int_0^{t_3} dt_4 \int_0^{t_4} dt_5 \int_0^{t_5} dt_6 E(p) E(q) E(r) \times \\
&\quad \times \left[4p^2 R(t_1 - t_6, p) R(t_2 - t_5, q) R(t_3 - t_4, r) + \right. \\
&\quad \quad 4p^2 R(t_1 - t_6, p) R(t_2 - t_4, q) R(t_3 - t_5, r) + \\
&\quad \quad 4p^2 R(t_1 - t_6, p) R(t_2 - t_3, q) R(t_4 - t_5, r) + \\
&\quad \quad (2p^2 + 2q^2) R(t_1 - t_5, p) R(t_2 - t_6, q) R(t_3 - t_4, r) + \\
&\quad \quad (p^2 + 2q^2) R(t_1 - t_4, p) R(t_2 - t_6, q) R(t_3 - t_5, r) + \\
&\quad \quad 2q^2 R(t_1 - t_3, p) R(t_2 - t_6, q) R(t_4 - t_5, r) + \\
&\quad \quad (2p^2 + r^2) R(t_1 - t_5, p) R(t_2 - t_4, q) R(t_3 - t_6, r) + \\
&\quad \quad (p^2 + q^2 + r^2) R(t_1 - t_4, p) R(t_2 - t_5, q) R(t_3 - t_6, r) + \\
&\quad \quad 2p^2 R(t_1 - t_5, p) R(t_2 - t_3, q) R(t_4 - t_6, r) + \\
&\quad \quad \left. q^2 R(t_1 - t_3, p) R(t_2 - t_5, q) R(t_4 - t_6, r) \right]
\end{aligned}$$

In two dimensions, the corresponding expressions are:

$$\begin{aligned}
D_2^{2D} &= \int_0^t dt_1 \int_0^{t_1} dt_2 \int_0^\infty dp E(p) R(t_1 - t_2, p) \\
D_4^{2D} &= -\frac{1}{2} \int_0^t dt_1 \int_0^{t_1} dt_2 \int_0^{t_2} dt_3 \int_0^{t_3} dt_4 \int_0^\infty dp \int_0^\infty dq p^2 E(p) E(q) R(t_1 - t_4, p) R(t_2 - t_3, q) \\
D_6^{2D} &= \int_0^\infty dp \int_0^\infty dq \int_0^\infty dr \int_0^t dt_1 \int_0^{t_1} dt_2 \int_0^{t_2} dt_3 \int_0^{t_3} dt_4 \int_0^{t_4} dt_5 \int_0^{t_5} dt_6 E(p) E(q) E(r) \times \\
&\quad \times \left[\frac{p^4}{4} R(t_1 - t_6, p) R(t_2 - t_5, q) R(t_3 - t_4, r) + \right. \\
&\quad \quad \frac{p^2 q^2}{4} R(t_1 - t_6, p) R(t_2 - t_5, q) R(t_3 - t_4, r) + \\
&\quad \quad \frac{p^4}{4} R(t_1 - t_6, p) R(t_2 - t_4, q) R(t_3 - t_5, r) + \\
&\quad \quad \frac{p^4}{4} R(t_1 - t_6, p) R(t_2 - t_3, q) R(t_4 - t_5, r) - \\
&\quad \quad \frac{p^2 q^2}{8} R(t_1 - t_5, p) R(t_2 - t_6, q) R(t_3 - t_4, r) - \\
&\quad \quad \frac{p^2 q^2}{16} R(t_1 - t_4, p) R(t_2 - t_6, q) R(t_3 - t_5, r) - \\
&\quad \quad \frac{p^2 r^2}{16} R(t_1 - t_5, p) R(t_2 - t_4, q) R(t_3 - t_6, r) - \\
&\quad \quad \left. \frac{p^2 r^2}{16} R(t_1 - t_4, p) R(t_2 - t_5, q) R(t_3 - t_6, r) \right] \\
F_2^{2D} &= 0 \\
F_4^{2D} &= 0 \\
F_6^{2D} &= \frac{135}{256} F_6^{3D}
\end{aligned}$$

References

- [1] G. A. Baker, “*Essentials of Padé approximants*,” Academic Press, (1975).
- [2] M. S. Borgas and B. L. Sawford, “Stochastic equations with multifractal random increments for modeling turbulent dispersion,” *Phys. Fluids*, **A 6**, 618-633 (1994).
- [3] G. Falkovich, K. Gawedzki, and M. Vergassola, “Particles and fields in fluid turbulence,” *Rev. Mod. Phys.*, **73**, 913-975 (2001).
- [4] J. P. Gleeson, “A closure method for random advection of a passive scalar,” *Phys. Fluids*, **12**, 1472-1484 (2000).
- [5] D. L. Koch and E. S. G. Shaqfeh, “Averaged-equation and diagrammatic approximations to the average concentration of a tracer advected by a Gaussian random velocity field,” *Phys. Fluids*, **A 4**, 887-894 (1992).
- [6] R. H. Kraichnan, “Diffusion by a random velocity field,” *Phys. Fluids*, **13**, 22-31 (1970).

- [7] W. D. McComb, V. Shanmugasundaram and P. Hutchison, "Velocity-derivative skewness and two-time correlations of isotropic turbulence as predicted by the LET theory," *J. Fluid Mech.*, **208**, 91 (1989).
- [8] A. H. Nayfeh, "*Perturbation Methods*," section 7.4, Wiley Interscience, (1973).
- [9] B. L. Sawford and M. S. Borgas, "On the continuity of stochastic models for the Lagrangian velocity in turbulence," *Physica D*, **76**, 297-311 (1994).
- [10] G. I. Taylor, *Proc. London Math. Soc.*, **20**, 196 (1921).